Front. Earth Sci. 2011, 5(1): 1–13
DOI 10.1007/s11707-011-0160-7

FEATURE ARTICLE

How severe is the modern biotic crisis? —— A comparison of global change and biotic crisis between Permian-Triassic transition and modern times

Hongfu YIN (✉), Weihong HE, Shucheng XIE

Key Laboratory of Biogeology and Environmental Geology of Ministry of Education, China University of Geosciences, Wuhan 430073, China

Abstract A comparison of the modern condition with the Permian-Triassic Boundary (PTB) times was made to estimate how severe the modern biotic crisis is. About the global changes, the two periods are correlative in carbon dioxide concentration and carbon isotope negative excursion, UV strengthening, temperature increase, ocean acidification, and weathering enhancement. The following tendencies of biotic crises are also correlative: acceleration of extinction rates accompanied by parabolic curve of extinction with a turning interval representing the critical crisis; decline of the three main ecosystems: reefs, tropical rain forests and marine phytoplankton. It is also interesting to note that certain leading organism in both periods undergo accelerated evolution during the crisis. The comparison shows that the modern crisis is about at the turning point from decline to decimation. The extinction curve is now parabolic, and the extinction rate has been accelerated, but the decimation is not yet in real. This is also justified by the modern situation of the three main ecosystems. Modern biotic decline may worsen into decimation and mass extinction but may also get better and recover to ordinary evolution. Since human activities are the main cause of the deterioration of environments and organisms, mankind should be responsible and able to strive for the recovery of the crisis. For the future of mankind, *Homo sapiens* may become extinct, i.e., disappear without leaving descendants, or evolve into a new and more advanced species, i.e., disappear but leave descendants. For a better future, mankind should be conscious of the facing danger and act as a whole to save biodiversity and harmonize with the environments.

Keywords comparison, global change, biotic crisis, Permian-Triassic Boundary (PTB), modern times

Received August 12, 2010; accepted October 26, 2010

E-mail: hfyin@cug.edu.cn

1 Introduction

It is now a general consensus that the modern world is experiencing profound global change and biotic crisis. However, as the debate about the "Climate gate" shows, there are controversies concerning the extent of their severity. One of the basic problem lies in that the modern time is but merely a twinkling of the geologic time. We do not know the whole course of global change and biotic crisis, especially their consequences in the future. In this regard, researches on global changes and synchronous biotic crises in geological history are of important reference value, because they may show the whole process and provide hints on the causes and consequences of the changes and crises. The global changes at Permian-Triassic Boundary (PTB) or Paleozoic-Mesozoic Boundary is one of these events, and the synchronous mass extinction is the most severe and profound one in geological history. A research on the comparison of global changes and biotic crises between PTB and modern times is worthwhile doing. Because both the PTB and modern times belong to critical periods of the geological history with profound global changes and biotic crises, a correlation between the two would be beneficial to both sides. On one hand, the whole course of PTB global change and biotic extinction may serve as a revelation, which will inspire us of the *status quo* and the future of the earth and its organisms, thus prompt us to adjust the relationship between mankind and nature. On the other hand, the PTB time displays only the results of past global change and biotic extinction in a much more brief record compared with the recent record; it gives a general pattern but leaves a lot of imaginary space for the actual process and causality. In this aspect, researches of modern process and dynamics may provide valuable information by applying the principle of uniformitarianism to the PTB research, which is a hotspot and frontier of geological studies. We are aware that the causes

of the two critical periods are different and that the modern one is mainly due to human activities. However, because the process and initial influences are similar, by comparing with the past, the consequence in the near future would be more predicable so that the mankind may be able to act in advance so as to change the tendency before it becomes inevitable. The past is the key to the present; meanwhile, the present is also the key to the past.

2 Correlation of the global changes between the PTB and modern times

2.1 Carbon dioxide concentration [$\rho(CO_2)$] and negative shift of carbon isotope ($\delta^{13}C$)

As indicated by IPCC, 2007, mainly due to human activities, $\rho(CO_2)$ has increased from 270×10^{-6} to 330×10^{-6} within past 150 years. The most recent data is 391×10^{-6} now (April 2010, Mauna Loa CO_2 annual mean data from NOAA). Bulk $\delta^{13}C$ of the modern oceans oscillated by glacial-interglacial changes and did not show remarkable long-term negative shift. However, a multi-parameter mixing approach (MIX) to reconstruct the industrial-era (1765–1992) change in $\delta^{13}C$ of dissolved inorganic carbon revealed that the industrial-era near-surface (< 200 m) $\delta^{13}C$ change ranged from -0.8 ‰ in the subtropics to -0.4 ‰ to -0.2 ‰ north of 40°N (Sonnerup et al., 2007), so a negative shift of marine $\delta^{13}C$ seems existing at 10^2a scope. Negative shifts of $\delta^{13}C$, sometimes quite strong, also occur in recent terrestrial deposits (Xie et al., 2004a, b).

The same tendency happened during PTB time. Based on the known relationship between leaf stomatal abundance and growing-season CO_2 concentrations, Retallack (2002) measured the stomatal index of mid-Permian to late Triassic *Lepidopteris* and concluded that the Early Triassic $\rho(CO_2)$ was $3314 \times 10^{-6} \pm 1097 \times 10^{-6}$, nearly 10 times that of today, and 2 times the averaged Permian level. It should be noted however that, although the Early Triassic $\rho(CO_2)$ is much higher than modern time, its growth rate during PTB interval is only $< 0.01 \times 10^{-6}$ annually, whereas the growth rate of modern $\rho(CO_2)$ would be from 0.4×10^{-6} to 2×10^{-6} annually[1)].

The negative shift of $\delta^{13}C_{carb}$ during PTB time is recognized worldwide. After a relatively stable period in Changhsingian, all latest Changhsingian curves show an increasingly rapid decrease in values, becoming negative just below the PTB (Yin et al., 2007). The scope of the negative shift ranged from -0.65 ‰ (Xie et al., 2007) to -1.62 ‰ (Jin et al., 2000) at the Meishan GSSP section. Scope of stronger negative excursion may reach -5 ‰, e.g., in Shahreza, Iran (Korte et al., 2004). This ubiquitous feature is important because it marks the beginning of a profound global change just prior to the PTB.

2.2 Global warming

There is a discernible warming trend of the global surface temperature over the past 150 years (1950–2007), from around -0.3°C to $+0.5$°C (IPCC, 2007). It may be too rigid to attribute most, if not all, of the historical global warming to $\rho(CO_2)$ concentration, because there are arguments that since available ice core data indicate the temperature always lead the CO_2 changes, CO_2 could not be the driver. The most recent 150 a climate changes may be caused partially by CO_2 and partially by natural fluctuations.

Palaeotemperature increase from Latest Permian to Early Triassic has been reported from oxygen isotopic values ($\delta^{18}O$) of marine biogenic carbonate (Veizer et al., 2000). From Latest Permian to Earliest Triassic, the $\delta^{18}O$ shifted from $+0.5$ to -1.5 ‰, corresponding to 8°C of temperature rise. The warming trend was also echoed by estimation from the stomatal index (SI)[2)] of fossil leaves of *Lepidopteris*. According to SI, atmospheric CO_2 concentration reached maxima in the latest Permian and then decreased to a negative shift in Early Triassic (Retallack, 2001, 2002), which reflects a strong warming tendency in accordance with the $\delta^{18}O$ shift.

2.3 Ultraviolet (UV) radiation

UV with wavelength between 290–325 nm is the main part of UV that may damage the immune system of organisms, causing skin cancer and other diseases. The ozone layer absorbs most UV with wavelength below 300 nm and protects organisms from over-exposure to UV. However, ozone depletion, the Antarctic ozone hole and a decline of ozone layer since the late 1970s probably due to overuse of chlorofluorocarbons (CFCs), has increased the modern UV exposure (Alpen, 1998).

Based on mutagenesis of PTB palynomorphs, Visscher et al. (2004) suggested that excessive UV radiation may have caused the PTB biotic crisis, especially the land vegetation, and meanwhile accelerated the genesis of new lineages. The extensive volcanism during that interval produced enormous SO_2 and formed large volume of

1) The PTB $\rho(CO_2)$ growth rate. The $\rho(CO_2)$ difference during PTB is about 1500–2000 ppm according to figures in Retallack (2001, 2002); the updated duration of PTB strata is ca. 300 ka according to pers. comm. of Sam Bowling 2009, 11. The modern $\rho(CO2)$ growth rate: 0.4×10^{-6}/a is calculated from $(330-270)\times10^{-6}$/150a; 2×10^{-6}/a is from data of 2009 for Mauna Loa, Hawaii, NOAA)

2) *SI* (stomatal index) = 100 *Ns*/(*Ns* + *Ne*), where *Ns* is the number of stomates, and *Ne* is the number of epidermal cells in the same area of cuticle. There is an inverse relationship between atmospheric CO_2 concentration and stomatal density, so SI may serve as a palaeobarometer of atmospheric CO_2 during growth of fossil plant leaves

H_2SO_4 aerosols, which would in turn accelerate activities of chlorine-bearing compounds and deplete the ozone layer of the stratosphere, thus strengthened the UV radiation.

2.4 Ocean acidification and/or hypercapnia

One third of the atmospheric CO_2 will be absorbed by the oceans and become carbonate acid. The increased $\rho(CO_2)$ caused by human activities will accelerate the solution of CO_2 in seawater, change the vulnerable balance of modern seawater and decrease its pH value. Ocean acidification is thus called the 'evil twin of global warming'. Between 1751 and 1994, surface ocean pH is estimated to have decreased from approximately 8.179 to 8.104, a change of -0.075 on the logarithmic pH scale that corresponds to an increase of 18.9% in H^+ (acid) concentration (Key et al., 2004; Orr et al., 2005). By the first decade of the 21st century however, the net change in ocean pH levels relative to preindustrial level was about -0.11, representing an increase of some 30% in 'acidity' (ion concentration) in the world's oceans (Hall-Spencer et al., 2008). Based on 8-year dataset of seawater acidity, salinity, and temperature measured at the Tatoosh Island offshore Washington State, USA, Wootton et al. (2008) reported that the averaged growth rate of seawater acidification is more than 10 times that which had been predicted by climate simulation.

Ocean acidification has essential impacts to marine life. It threats calcification of organism shells, alterate the balance of ecosystem, and may cause major changes in dominant species and habitat types. It was set forth as one of the possible causes of PTB mass extinction (Payne et al., 2010). Liang (2002) reported that the 'white clay' of Bed 25 at the PTB of Meishan yields strong acidity. Its pH value from more than 100 samples ranges from 0.8–1.3, averaged 1.1. He further postulated that this represents residual acids from the PTB marine water. This suggestion was questioned because the extremely strong acidity (pH = 1.1) seems unlikely to happen in sea water, and because Bed 25 contains gypsum, the weathering of which under wet conditions should produce sulfuric acid. Based on the anomalous hopane distribution at the PTB of Meishan, Wang (2007) suggested that either these hopanes were originated from acidified soil and peat, or it was caused by freshening and acidification of the upper water column during the PTB time. However, such acidification, if it did exist during PTB, was not strong enough to hinder the widespread carbonate deposits, nor was there sufficient evidence of more vulnerable skeletal physiology during that interval.

Instead of acidification, Knoll et al. (2007) suggested that hypercapnia, the physiologic effects of elevated $\rho(CO_2)$, best explains the selective survival of marine invertebrates during PTB. O_2 and CO_2 diffuse similarly in air, but in water, CO_2 is about 28 times more soluble than O_2. Thus, marine animals are far more sensitive to hypercapnic stress than land vertebrates and plants. Answering the argument that calcified shelly fauna were able to flourish in geologic periods with high $\rho(CO_2)$, they emphasized that it is the rapid increase of $\rho(CO_2)$ during PTB time and not its absolute value that caused important associated changes, such as reduced $[CO_3^{2-}]$, pH, and carbonate saturation of seawater. Marked change over a few generations leaves populations little chance to produce adaptive characters for survival. Paleophysiological perspectives further suggest that persistent or recurring hypercapnia/global warmth also played a principal role in delayed Triassic recovery.

2.5 Aragonitic and high Mg/Ca seawater

In geologic history, there were three aragonitic seawater periods alternate by two calcitic seawater periods. The three aragonitic seawater periods are latest Pre-Cambrian–Early Cambrian, Late Carboniferous-Late Triassic, and Middle Cenozoic-recent (Sandberg, 1983). Yan and Wu (2006) showed that the PTB time was at the zenith of the second aragonitic seawater period, while the recent time is at the zenith of the third aragonitic seawater period. It is noticeable that the aragonitic-calcitic circle show temporal accordance with the circle of evaporates. Evaporites of $MgSO_4$ type highlights during aragonitic periods, while evaporates of KCl type dominates during calcitic periods. Phanerozoic oscillations in the $x(Mg)/x(Ca)$ ratios of seawater and the preliminary mineralogy of marine carbonates and evaporites are synchronized. This corresponding change was interpreted as concordant oscillation of the chemical composition of seawater controlled by growth rates of ocean ridges (Yan and Wu, 2006). Change of the chemical composition of seawater exerts profound influence on the relative development of shelly fauna with different carbonate (or magnesium) compositions. Usually, the transition period from one type of seawater composition to the other type is the critical time for organisms and may lead to biotic crisis or extinction. For example, PTB and Precambrian-Cambrian intervals are such transitional periods of seawater composition; meanwhile, they are also critical periods for evolution. Applying the Mg/Ca curve of Horita et al. (2002), Yan and Wu have suggested that following the ascending of Mg/Ca and increase of aragonitic content, the Permian shelly faunas with low Mg/Ca calcitic shells, such as rugose and tabulate corals, fusulinids, brachiopods, and bryozoans, rapidly decimated one by one (Table 1), because the shift of seawater composition evidently impeded their shell growth. The Mg/Ca ratio and aragonitic content descended since Early Triassic, and it is echoed by the successive recovery of, at first, aragonitic shelly faunas, such as ammonoids, bivalves, and gastropods. The calcitic shelly faunas like brachiopods and bryozoans only recovered by the Middle Triassic when Ca has been accumulated enough, and the Mesozoic corals has changed into aragonitic frame—sclerctinian corals. The validity of their suggestion should be tested for the change of modern biota, because the

Table 1 Diversities of Permian-Triassic marine invertebrate genera in South China (modified from Yin et al., 2007)

Taxa	Early Permian			Late Permian		Early Triassic		
	AA	KR	RC	W	C	I	O	A
Fusulinids	60	45	75	15	8	0	0	0
Non-fusulinid foraminifers	34	42	44	37	44	13	22	39
Corals	94	83	97	19	9	0	0	0
Brachiopods	49	78	82/61	82/29	83	12	3	41
Ammonoids			37	28	43	24	77	51

Abbreviations: AA: Asselian–Artinskian; KR: Kungurian + Lower Roadian; RC: Upper Roadian– Capitanian; W: Wuchiapingian; C:Changhsingian; I: Induan; O: Olenekian; A: Anisian; 82/61 are numbers of taxa in lower stage/upper stage, respectively

modern seawater composition is cycling back to mimic that of PTB time, and similar processes should be ongoing in the shelly faunas.

2.6 Other similarities and predictable tendencies

2.6.1 Enhanced weathering on land

Following the deforestation, enhanced aridity, and greenhouse effect, strengthened continental weathering have been recorded in PTB time (Ward et al., 2000). At Graphite Peak, Antarctica, relative to the latest Permian paleosols, the earliest Triassic paleosol exhibits greater leaching, greater accumulation of immobile REEs, and evidence of lower soil ρO_2. These results support a rapid shift (perhaps 10000 year) to an earliest Triassic enhanced weathering (Sheldon, 2006).

With accelerated deforestation and global warming, it is predictable that more rapid release of large quantities of carbon into the ocean-atmosphere system will be triggered due to this intense episode of dissolution. Enhanced continental weathering/runoff and carbonate precipitation will occur. This has been recorded regionally in modern world (Li et al., 2005).

2.6.2 Stagnant and disoxic ocean

During PTB, stagnant and disoxic water mass was widespread (Grice et al., 2005; Huang et al., 2007). The global anoxia was regarded as a major cause of PTB mass extinction (Hotinski et al., 2001 and many others). The modern Black Sea has a much fresher surface water due to fluvial inputs; the deep waters do not mix with the upper layers of water that receive oxygen from the atmosphere. As a result, over 90% of the deeper Black Sea volume is anoxic water. So far, marine anoxia only develops regionally in the modern world, but with temperature rise of surface water and oxygen consumption by over-nutritious fresh flow, disoxic stratified water mass may become more developed in marine environment.

2.6.3 Pollution of metal elements

The PTB witnessed a concentration of pollutant metals at the extinction horizon (Yang et al., 1993; Yu et al., 2007). This was regarded by some as evidence of extraterrestrial origin (Chai et al., 1992). Pollution of metal elements in modern deposits has been repeatedly reported mainly due to contamination of industry waste, and the tendency will continue for decades.

2.7 Environmental instability

The modern earth's surface system is under great environmental instability. Global warming, atmospheric change, water pollution, sea level rising, natural disaster strengthening, loss of forest and agricultural land, biodiversity crisis, and ecosystem breakdown, all these can be attributed mainly or partly to human influences. The paleo-environment of the PTB world was also a remarkably unstable one, and most of the modern environmental disturbances also occurred during that interval (Huang et al., 2007; Payne et al., 2004; Tong et al., 2007). To sum up, the correlation of the global changes between the PTB and modern times reveals a general tendency toward environmental deterioration and crisis of both. However, the extent of modern deterioration is less severe or still in the initial stage. This stands for the $\rho(CO_2)$ concentration, the global warming, and the ocean anoxia. Mankind is still barely in time to prevent an environmental collapse.

3 Correlation of the biotic crisis between the PTB and modern times

3.1 Extinction rate

Based on data from World Conservation Monitoring Centre (WCMC) and other resources, Groombridge (1992) provided the extinction curve, mainly on vertebrate animals, since 1960 (Fig. 1). The general pattern is a parabolic curve with turning point around 1850,

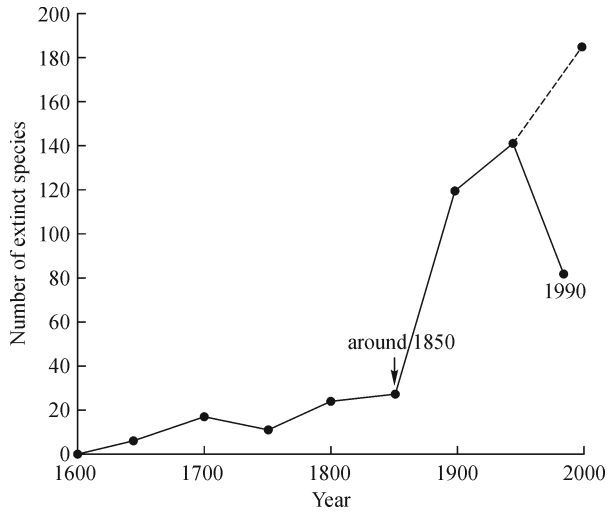

Fig. 1 Broken-line graph of animal extinction. Solid broken lines (1600–1990) are from Groombridge (1992); dotted line is based on indication from Butchart et al. (2010)

representing the acceleration of extinction in industry-age. In Fig. 1, the rate suddenly goes downward in the 1950–1990 period, which was suggested by some authors as a progress that resulted from conscious remedial measures taken by the government to protect biodiversity (Smith et al., 1993). This suggestion is highly improbable. The downward segment should be caused mainly by the definition of extinction given by documents of the Convention on International Trade in Endangered Species of Wild Fauna and Flora (CITES), in which 'extinction' was defined as nondiscovery of a species in field continuously for a 50 a duration. It is thus impossible to count species disappeared since 1950 as 'extinct' because in 1992, the disappearance is less than 50 a. Butchart et al. (2010) compiled 31 indicators to estimate the rate of biodiversity loss in past 50 a (1970–2010). 'Most indicators of the state of biodiversity (covering species' population trends, extinction risk, habitat extent and condition, and community composition) showed declines, with no significant recent reductions in rate.' Meanwhile, indicators of pressures on biodiversity showed increases. They concluded that the rate of biodiversity loss does not appear to be slowing in the past 50 a. Unlike the Groombridge (1992) graph where the 1950–1990 extinction line decelerated, they reported that the mean population trends of vertebrates show a decline of 31% since 1970, as shown by the dotted line in Fig. 1.

There are two ways to estimate the extinction rate acceleration. One way is by comparison between actual and background numbers of extinct species. The background extinction rate known from the fossil record is about one species per million species per year or between 10 and 100 species per year altogether (counting all organisms). About the actual numbers, Wilson (1992) estimates that 27000 species are currently lost per year and stressed that by 2022, 22% of all species will extinct if no action is taken. Eldredge (1998) estimates 30000 per year currently. These estimates place the extinction rate at 300–3000 times the background rate. According to Butchart et al. (2010), the vertebrates decline (-31% since 1970) will have an even quicker rate. A conservative estimation is about 1000 times the background rate (Heywood, 1995).

The other way is by comparison between actual extinction rate and background extinction rate of certain organism group. According to WCMC, 229 species of vertebrate have become extinct since 1600. Current vertebrate species numbers are 3.7×10^4 (Smith et al., 1993). Given the averaged 'lifespan' of a vertebrate species as 5 Ma, the extinction rate of current vertebrates would be 75 times of their background extinction rate (He et al., 2004). Mammals, for instance, have an average species "lifespan" from origin to extinction of about 1 million years. There are about 5000 known mammalian species alive at present. Given the average species 'lifespan' for mammals, the background extinction rate for this group would be approximately one species lost every 200 a. Nevertheless, the past 400 a have seen 89 mammalian extinctions, almost 45 times the predicted rate.

Based on data from Jin et al. (2000), 98 out of 160 species became extinct at the GSSP Meishan section during the main phase of end-Permian mass extinction (251.45–251.20 Ma). Given the "lifespan" of marine invertebrate species as 10 Ma, the end-Permian extinction rate would be 25 times the background rate (He et al., 2004).

The accelerated extinction rates of these two periods undoubtedly suggest that both are in the midst of a mass extinction. The modern extinction rate seems even larger than that of the PTB time. The difference of rate acceleration between the two may be due to that the actual extinction rate is difficult to pin down with shorter time or that the PTB rate is underestimated due to lack of large number sampling and precise time span assessment. If the rate difference is true, it can be explained that anthropogenic changes may be much more rapid than natural changes.

The extinction curve since 1600 has been published based on statistics of extinct species given by WCMC (Groombridge, 1992). A curve of relative extinction rates during PTB and modern times was given (Table 2, Fig. 2). Although direct temporal correlation is impossible because of the disparate time scale of the two intervals, Fig. 2 does show correlative tendencies of extinction curves. Comparison of stage-subdivision of the Permian-Triassic mass extinction with that of current species extinction shows that the modern curve is similar to the preludial part of the PTB curve. It verifies that extinction rates are increasing in an antiparabolic curve in marine and terrestrial ecosystems around the world in recent centuries, and the modern time is experiencing the initial stage of extinction. We have also used the method of 'species-area curve' (Dobson, 1996) to

Table 2 Number of extinct species and genera and their extinction rates of PTB time in South China (modified after He et al., 2004)

Geological age/Ma	Extinct species	Extinction rate/(species·Ma^{-1})	Extinct genera	Extinction rate/(genera·Ma^{-1})
253.4–253.0	33	83	131	66
253.0–252.3	73	104	131	66
252.3–52.0	12	40	131	66
252.0– 251.4	43	72	131	66
251.4–251.2	98	490	93	465
251.2–251.0	11	55	38	63
251.0–250.6	27	68	38	63
250.6–250.4	5	25	38	63

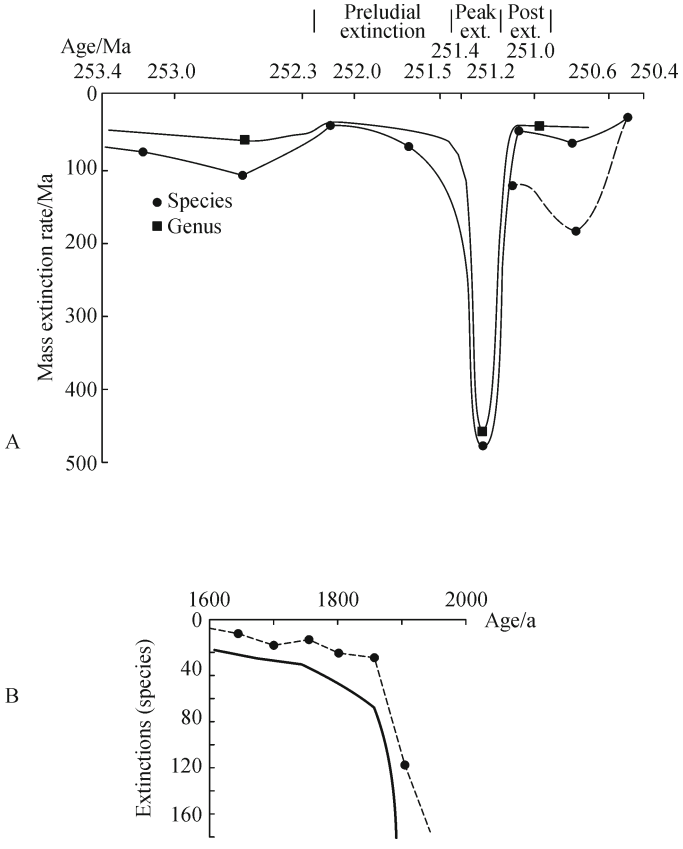

Fig. 2 Comparison of extinction curves between the PTB extinction (A, invertebrates) and modern extinction (B, solid line-animals, dotted-all organisms) (modified after He et al., 2004). The abscissa of A represents the ages of each segment of Meishan section (Ma). Bed 25-Bed 28 is 251.4 –250.6, data from Jin et al. (2000). Now that the duration may be shortened (Bed 25-Bed 28 is 252.40 –252.12, S. Bowling pers. comm.), and the second phase of extinction at Bed 28 should be stronger than the solid line (Xie et al., 2005; Yin et al., 2007); the curve may have to be modified as drafted by the dashed line (not based on statistics), in which the second phase becomes a negative excursion.

cross check the results of modern diversity loss and forest area decrease in Asia, Africa, and Latin America (Tables 3 and 4), and reached the same conclusion. 'The Earth is now in the midst of its first great extinction event caused by the activities of a single biologic species (humankind)'. (Steffen et al., 2004).

Table 3 Preliminary estimation of forest area and forest cleared situation in Asia, Africa, and Latin America (Groombridge, 1992)

Area	Forest area/km^2		Forest cleared area/km^2			
	1980	1990	Pre-1650	1650–1749	1750–1849	1850–1978
Asia	3108000	2748000	807	196	601	1220
Africa	6504000	6001000	161	52	13	469
Latin America	9229000	8399000	15	100	170	637

Table 4 Numbers of erosional species and their erosional rate in forest areas of Asia, Africa, and Latin America

Area	Erosional species					Erosional rate/(species·s^{-1})				
	ΔS (pre-1650)	ΔS (1650 – 1750)	ΔS (1650 – 1850)	ΔS (1650 – 1980)	ΔS (1650 – 1990)	pre-1650	1650 – 1750	1750 – 1850	1850 – 1980	1980 – 1990
Asia	$0.005\ S_{03}$	$0.01\ S_{03}$	$0.04\ S_{03}$	$0.12\ S_{03}$	$0.14\ S_{03}$	$<4\times10^{-6}S_{03}$	$1\times10^{-4}S_{03}$	$3\times10^{-4}S_{03}$	$6\times10^{-4}S_{03}$	$2\times10^{-3}S_{03}$
Africa	$0.008\ S_{02}$	$0.002\ S_{02}$	$0.003\ S_{02}$	$0.02\ S_{02}$	$0.04\ S_{02}$	$<5\times10^{-6}S_{02}$	$2\times10^{-5}S_{02}$	$1\times10^{-5}S_{02}$	$1\times10^{-4}S_{02}$	$2\times10^{-3}S_{02}$
Latin America	$0.001\ S_{01}$	$0.003\ S_{01}$	$0.01\ S_{01}$	$0.023\ S_{01}$	$0.05\ S_{01}$	$<1\times10^{-6}S_{01}$	$3\times10^{-5}S_{01}$	$7\times10^{-5}S_{01}$	$1\times10^{-4}S_{01}$	$2.7\times10^{-3}S_{01}$

3.2 Crises of the three essential ecosystems

Marine phytoplankton, reef, and tropical forest are the three major and most diversified ecosystems of modern world. Essentially, the same situation existed during the Permian time (Erwin, 1993), so this provides another good parameter for comparison.

3.2.1 Reef

The Great Barrier Reef along the coast of Australia experienced 7 bleaching events during 1980–2006. The most widespread and intense events occurred there in the summers of 1998 and 2002, affecting about 42% and 54% of reefs, respectively. Many other coral reef provinces have been permanently damaged by warm sea water temperature, most severely in the Indian Ocean. Up to 90% of coral cover has been lost in the Maldives, Sri Lanka, Kenya and Tanzania, and in the Seychelles (Parry et al., 2007). In the period of 2010–2040, coral reefs are expected to become highly susceptible to more frequent bleaching events. The IPCC (2007) sees this as the greatest threat to the world's reef systems. Butchart et al. (2010) reported a 38% decline of coral reef condition (live hard coral cover) during 1980–2004.

3.2.2 Tropical forest

Global deforestation sharply accelerated around 1852. Tropical rainforest is now seriously fragmented and locally disappeared (FAO, 2001; He et al., 2004). It has been estimated that about half of the Earth's mature tropical forests, between 7.5×10^6 and 8×10^6 km^2 of the original 15×10^6 to 16×10^6 km^2 that has covered the planet until 1947 have now been cleared. Some scientists have predicted that unless significant measures are taken on a worldwide basis, by 2030, there will only be ten percent remaining (Nielsen, 2006), with another ten percent in a declining condition. 80% will have been lost, and with them, hundreds of thousands of irreplaceable species (Wilson, 2002). A 2005 report by the United Nations Food and Agriculture Organization (FAO, 2005) estimates that the Earth's total forest area continues to decrease at about 13×10^6 ha/year. Butchart et al. (2010) reported a 3.1% decline of forest extent in 1990–2005.

We have attempted to calculate the acceleration rate of deforestation, using the method of species-area curve (Dobson, 1996), based on preliminary estimations of forest area (1980–1990) and forest cleared situation (pre-1650 to around 1980) in Asia, Africa, and Latin America (Table 3; Groombridge, 1992).

From the species-area curve, we have

$$S = cA^z. \tag{1}$$

Thus

$$S_{01} = cA_1^z, \tag{2}$$

$$S_{02} = cA_2^z, \tag{3}$$

$$S_{03} = cA_3^z. \tag{4}$$

A_1, A_2, and A_3 denote the forest area of Asia, Africa, and Latin America in 1650, respectively. S_{01}, S_{02}, and S_{03} denote the number of species in the forest area A_1, A_2, and A_3, respectively.

Thus, we also have

$$\Delta S = S_{0i} - S'_{0i} = (1 - (A'_i / A_i)^{0.25}) S_{0i}, \quad (5)$$

where i = 1, 2, 3; A' is for the different forest areas of different periods; S'_{0i} is for the species number of forest A'_i ; ΔS is for the differential value of species numbers when the forest area shifted from A_i to A'_i .

The erosion of species (erosion ≈ disappearance) in different periods and the erosional rate of species can thus be calculated by substituting the numbers of Table 3 into Formula 5. Thus, we have the numbers of erosional species and their erosional rate in Asia, Africa, and Latin America, as expressed in Table 4. It is clear from the tables that both the rate of deforestation, the erosion of species, and the rate of species erosion following deforestation are accelerating since 1650. Figure 3 shows the rate of erosional species in an Asian forest based on Groombridge (1992) that shows an acceleration anto-parabolic curve of extinction (erosion). Those of Africa and Latin America show more or less the same tendency (He et al., 2004). These echoes with the animal extinction during the same interval.

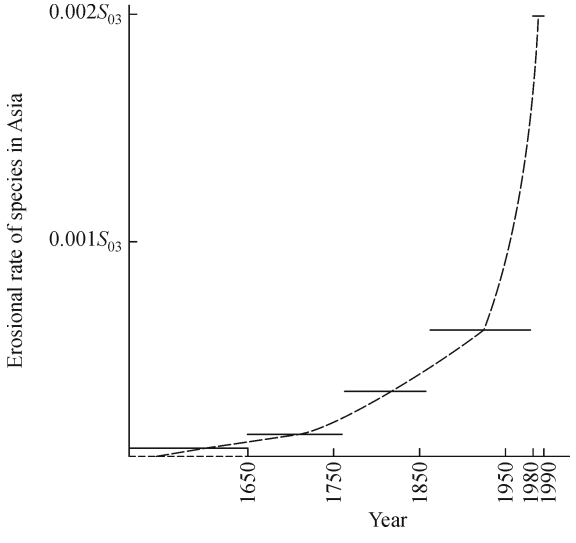

Fig. 3 Rate of erosional species in Asian forests (based on Groombridge, 1992). Based on data from Table 4, transverse bars: annual rate of erosional species in each time interval; dotted line: general tendency of erosional rate

3.2.3 Marine phytoplankton

It is to be noted that, in contrast to the macro-organisms, microbes do not decline when the environment begins to deteriorate. When the oxygen deficiency of water bodies worsens, usually, the microbes shift in the following succession: slightly disaerobic — photosynthetic and aerobic microbes (e.g., cyanobacteria) flourish; disaerobic — they decline; quasi-anaerobic — sulfur reduction bacteria (SRB) flourish; and anaerobic — methanogenic bacteria flourishes. Flourishing of SRB and methanogens would mean widespread anoxia in the ocean, occurring only in the earth's early history and extreme deteriorated environments in Phanerozoic, as during the PTB time (Huang et al., 2007). In the modern world, there are lots of regional microbial flourish where the water bodies become over nutritious or polluted by heavy metals, some of which like Fe are necessary for microbe growth. Microbial blooms occur frequently in marginal seas, river mouths, and lakes of many regions in the world. On the other hand, the global decline of photosynthetic and aerobic microbes seems likely to have begun in modern oceans. Applying combined data of ocean transparency measurements and in situ chlorophyll observations available since 1899, Boyce et al. (2010) observed marine phytoplankton declines in eight out of ten ocean regions and estimated a global rate of decline of ~1% per year. Behrenfeld et al. (2006) have reported earlier that the marine primary productivity had a declining tendency (1999–2006) after a short time (1998–1999) of increase.

3.2.4 Fate of the three major ecosystems during the PTB time

Permian is a period of coal accumulation, most of which are from tropical rain forest constituted by lycopodiales and gymnosperms. Porifers, rugose, and tabulate corals dominated shallow water habitats and build huge reefs. Phytoplankton, although difficult to find in fossil, should be very abundant judging from the high primary productivity (PP) of that period. The three major ecosystems collapsed abruptly at the end-Permian mass extinction. There were three famous gaps: coal gap, reef gap, and silicolite gap in the Early Triassic. The coal gap and reef gap indicates the decimation of forests (esp. tropical rainforests) and reefs. Among the three, reef ecosystem became extinct first (Stanley, 2001). Tropical forest disappeared later, and the last *Gigantopteris* flora survived until earliest Triassic (Yu et al., 2007). Silicolite gap means decimation of radiolarians, which may imply decline of phytoplankton on which they fed. When the macro-organisms became extinct, one of the main primary producers, cyanobacteria, flourished at first (Wang et al., 2005; Xie et al., 2005), then wax and wane frequently during the PTB interval, and its flourish and decline reciprocally alternate with that of the SRB (Huang et al., 2007; Luo et al., 2010). This phenomenon represented an instability situation of redox conditions in the global shallow water, and the latter severely shrank the base of marine ecosystem to the extent that there may be a global

euxinic condition (Grice et al., 2005). *Reduviasporites* (or *Tympanicysta*), a disastrous species of fungal or palynomorph origin, boomed in both marine and continental circumstances when the main extinction event happened (Visscher et al., 1996).

The end-Permian mass extinction is called the most severe one of the 'Big Five' mass extinction in Phanerozoic or the 'Mother of Mass Extinctions" (Erwin, 1993). This is not only because its biodiversity loss is the biggest (> 90% at species level) and its recovery interval is the longest (ca. 5 Ma) but also because its ecosystem collapse is the most profound. Not only did the higher rank organisms of the ecosystem hierarchy decimate, but also the microbes that constitute the base of the pyramid severely shrunk. In this regard, the present biotic crisis is much lighter in comparison with the PTB one; because the reefs are bleached but only partly disappeared, the rainforest are fragmented but not overall decimated, and instead of shrinking, the microbes are still blooming in over-nutritious water bodies.

3.3 Evolutionary acceleration of certain ruling organisms

The average duration per conodont zone is about 300 ka in Permian (18 zones in 50 Ma), 100 ka in Late Permian (10 zones in 10 Ma), and nearly 800 ka in Early Triassic (8 zones in 6 Ma) (Gradstein et al., 2004). However, the PTB conodont zonation is much denser. At the GSSP Meishan section (Jiang et al., 2007) and at the Abadeh section of Iran (Kozur, 2007), numbers of conodont zones within the PTB interval (corresponding to Beds 25–28 at Meishan) is 5 and 7, respectively. Given 300 ka for that time span, the duration per conodont zone of PTB would be only 40–60 ka. This is unlikely to be a result of sampling bias because both the Late Permian and Early Triassic conodont zonations have been collected in detail and correlative world-wide. This temporal shortening of PTB conodont zones should indicate evolutionary acceleration of conodontophora animals as a survival strategy to adapt to the strengthening stress of PTB environmental crisis. Likewise, condensed radiolarian zonation at PTB was also reported in South China.

The time line of hominoid species shows a clear tendency of accelerated evolution of species and subspecies since 5 Ma ago. The four *Australopithecus* species have an average 'lifespan' of 1.10 Ma, the three *Homo* species averaged 0.87 Ma, while *Homo sapiens* and its subspecies averaged 0.17 Ma (up to now).

Australopithecus ramidus–5 to 4 million years BC
Australopithecus afarensis–4 to 2.7 million years BC
Australopithecus africanus–3.0 to 2.0 million years BC
Australopithecus robustus–2.2 to 1.0 million years BC
Homo habilis–2.2 to 1.6 million years BC
Homo erectus–2 to 0.4 million years BC
Homo sapiens–400000 to 200000 years BC
Homo sapiens neandertalensis–200000 to 30000 years BC
Homo sapiens sapiens–130000 years BC to present

Using the 3.9-million HapMap SNP dataset, Hawks et al. (2007) found that the positive selection of *H. sapiens sapiens* has accelerated greatly since the Neolithic time. Based on genomic surveys of 270 human individuals, including European ancestry, African (Yoruba) ancestry, Han Chinese, and Japanese, they concluded that during the past 40000 years, the rate of human's adaptive evolution has been 100 times higher than the ordinary rate that characterized most of human evolution. They suggested that the human population growth generated more new selected mutations. Population growth and the past changes in human cultures and ecologies may have contributed to the extraordinarily rapid recent genetic evolution of our species.

It may be interesting to note that both conodonts (Phyllum Chordata) and hominoids are leading, and index animals of respective geologic periods and conodonts survived the PTB crisis with accelerated evolution. This may be a coincidence but worthwhile to mention for further notice.

4 Correlativity of the global changes and biotic crises of the two periods

One major difference of the two periods is the cause of global changes and biotic crises. It is common sense that the modern ones are mainly anthropogenic. Aside from a bolide impact, which is still a hypothesis, intensive volcanism is widely accepted as a main cause that triggered the PTB global changes and biotic crises (Yin et al., 1992; Racki, 2003). However, given this difference in causality, the effects of PTB volcanism and modern human activities modern are largely similar and correlative: increase of $\rho(CO_2)$ and $\rho(SO_2)$ in atmosphere, greenhouse effect and ocean acidification, collapse of the basic ecosystems, etc.

Another major difference of the two periods is their disparate time range. The PTB duration has been estimated from less that 10 ka (Rampino et al., 2000) to nearly 0.7 Ma (Bowring et al., 1998). Using the high-precision LD-TIMS, recent data given in a Nov. 2009 meeting in Nanjing (Bowring S., pers. comm.) showed that it was about 0.3 Ma. This is far too long in duration compared with the 300 years of anthropogenic activities in industry-age. Any modern curve put in the PTB scale will become extremely short but with greater steepness, or nearly vertical direction; on the other hand, any PTB curve put in modern 10^2a scale will become nearly horizontal, no matter how intensive it was with geological viewpoint. However, environmental and biotic curves spanning the two periods respectively have one essential phenomenon

in common, i.e., both have parabolic patterns representing accelerated tendency of deterioration across a turning point (or short interval). In the modern time (1750–2000), such patterns have been shown in atmosphere (CO_2, N_2O, CH_4, and ozone depletion), climate (temperature and floods), coastal zone, ocean, and terrestrial ecosystems, and global biodiversity (Steffen et al., 2004). The same can be applied to the PTB time for atmosphere and temperature (Veizer et al., 2000; Retallack, 2001, 2002), seawater composition (Yan and Wu, 2006), and global biodiversity (Sepkoski, 1992). The similarity in their temporal curve denotes that both are critical periods in geological history and have experienced or is experiencing profound changes in the earth's surface system and organism evolution. As the Executive summary of IGBP (Steffen et al., 2004) put it, "The Earth is currently operating in a no-analogue state. The nature of changes now occurring simultaneously in the Earth system, their magnitudes, and rates of change are unprecedented in human history and perhaps in the history of the Earth. Extinction rates are increasing sharply in marine and terrestrial ecosystems around the world."

5 Conclusions

1) Although the causes and time spans of PTB and modern global changes and biotic crises are different, the two periods are correlative in the following tendencies of global changes: carbon dioxide concentration [$\rho(CO_2)$] and carbon isotope ($\delta^{13}C$) excursion, UV strengthening, temperature increase, ocean acidification/hypercapnia, and terrestrial weathering enhancement.

2) The following tendencies of biotic crises are correlative: Acceleration of extinction rates accompanied by parabolic curve of extinction with a turning interval representing the critical crisis; decline of the three main ecosystems, namely, reefs, tropical rain forests, and marine phytoplankton. It is also interesting to note that certain leading taxa of organisms underwent accelerated evolution during the crisis and survived.

3) The PTB crisis went through all the substages of mass extinction: decline, decimation, survival, and recovery. A comparison on the extent of biotic crises between the two periods shows that the modern crisis is about at the turning point from decline to decimation (Fig. 2). The extinction curve is now parabolic, and the extinction rate has been accelerated, but the decimation is not yet realized. This is also justified by the modern situation of the three major ecosystems: The reefs are bleaching but have not collapsed; the tropical forests are fragmented, but not yet decimated; the marine phytoplanktons are having blooms and are only just about to decline.

4) Modern biotic decline may worsen into decimation and undergo mass extinction but also may get better and recover to ordinary evolution. In the latter case, a mass extinction is not performed, and the biotic crisis will become a downward excursion of the future evolutionary curve. There are always oscillations of extinction and origination curves in the geological history. We are not sure whether the present biotic crisis will inevitably turn into a mass extinction or just form a downward oscillation of the curve. Since human activities are the main cause of the deterioration of environments and organisms, mankind should be responsible and able to strive for the better result — recover the crisis.

5) As to mankind himself, it seems very probable that human being as a species is experiencing an accelerating evolution. Since populations of *Homo sapiens sapiens* are developing new genomes 100 times faster than its ordinary evolution pace, as Hawks et al. (2007) said, this species is more than ever rapidly to disappear. There are two possibilities for the future of mankind. If the human-caused mass extinction becomes true, *Homo sapiens sapiens* may become extinct, i.e., disappear without leaving descendants. In geological history, it generally happened that the leading organisms would be decimated or become extinct during mass extinction, thus opened a new era dominated by new leading taxa. This is true for the DDO graptolites (Dicranograptidae, Diplograptidae, and Orthograptidae; Melchin and Mitchell, 1991) of the Late Ordovician mass extinction, the rugose and tabulate corals and fusulinids of the PTB mass extinction (Table 1), the ceratitid ammonoids and conodonts of the end-Triassic mass extinction and the dinosaurs and ammonoids of the end-Cretaceous mass extinction. Now that the human being is the leading organism, the main target and sacrifice of the coming mass extinction would have to be the *Homo* species. However, there is the other possibility that *H. sapiens* may quickly evolve into a new and more advanced species, i.e., disappear but leave descendants, as the conodonts have done to survive the PTB extinction. This happened in the earlier evolutionary history of hominids. Through long-term adaptive struggle with environments, *Australopithecus* developed both its physical and mental strength. Its brain enlarged, its vertebra straightened; in the course of labor, it became *Homo* and disappeared for itself. The essential difference between mankind and other organisms is that mankind has an intellectual mind. It is fully possible that mankind will become conscious of facing danger and act as a whole to save biodiversity and harmonize with the environments. The future is hopeful, but we need to take action now.

Acknowledgements This work is financially supported by the National Natural Science Foundation Program for Innovative Research Team of China (Grant No. 40921062), the National Natural Science Foundation of China (Grant Nos. 40930210, 40872008), and the Ministry of Education of China (NCET-10-0712). Many results of this paper came from fruitful discussions with colleagues of the BGEG Laboratory.

References

Alpen E L (1998). Radiation Biophysics. New York: Academic, 2nd ed, 484

Behrenfeld M J, O'Malley R T, Siegel D A, McClain C R, Sarmiento J L, Feldman G C, Milligan A J, Falkowski P G, Letelier R M, Boss E S (2006). Climate-driven trends in contemporary ocean productivity. Nature, 444(7120): 752–755

Bowring S A, Erwin D H, Jin Y G, Martin M W, Davidek K, Wang W (1998). U/Pb zircon geochronology and tempo of the end-permian mass extinction. Science, 280(5366): 1039–1045

Boyce D G, Lewis M R, Worm B (2010). Global phytoplankton decline over the past century. Nature, 466: 591–596

Butchart S H M, Walpole M, Collen B, van Strien A, Scharlemann J P W, Almond R E A, Baillie J E M, Bomhard B, Brown C, Bruno J, Carpenter K E, Carr G M, Chanson J, Chenery A M, Csirke J, Davidson N C, Dentener F, Foster M, Galli A, Galloway J N, Genovesi P, Gregory R D, Hockings M, Kapos V, Lamarque J F, Leverington F, Loh J, McGeoch M A, McRae L, Minasyan A, Morcillo M H, Oldfield T E E, Pauly D, Quader S, Revenga C, Sauer J R, Skolnik B, Spear D, Stanwell-Smith D, Stuart S N, Symes A, Tierney M, Tyrrell T D, Vie J C, Watson R (2010). Global biodiversity: indicators of recent declines. Science, 328(5982): 1164–1168

Chai C F, Zhou Y Q, Mao X Y, Ma S L, Kong P, He J W (1992). Geochemical constraints on the Permo-Triassic boundary event in South China. In: Sweet W C, Yang Z Y, Dickins J M, Yin H F, eds. Permo-Triassic Events in the Eastern Tethys. Cambridge: Cambridge University Press, 158–168

Dobson A P (1996). Conservation and Biodiversity. New York: Scientific American Library, Freeman & Co

Eldredge N (1998). Life in the Balance: Humanity and the Biodiversity Crisis. Princeton: Princeton University Press, 240

Erwin D H (1993). The Great Paleozoic Crisis: Life and Death in the Permian. New York: Columbia University Press, 327

Food and Agriculture Organization of the United Nations (FAO) (2001). State of the World's Forests. Rome: FAO

Food and Agriculture Organization of the United Nations (FAO) (2005). "Pan-tropical Survey of Forest Cover Changes 1980–2000". In: Forest Resources Assessment. Rome: FAO

Gradstein F, Ogg J, Smith A (2004). A Geologic Time Scale. London: Cambridge University Press, 589

Grice K, Cao C Q, Love G D, Böttcher M E, Twitchett R J, Grosjean E, Summons R E, Turgeon S C, Dunning W, Jin Y (2005). Photic zone euxinia during the Permian-triassic superanoxic event. Science, 307 (5710): 706–709

Groombridge B (1992). Global biodiversity-status of the Earth's living resources. A Report Compiled by the World Conservation Monitoring Center. London: Chapman & Hall, 192–265

Hall-Spencer J M, Rodolfo-Metalpa R, Martin S, Ransome E, Fine M, Turner S M, Rowley S J, Tedesco D, Buia M C (2008). Volcanic carbon dioxide vents show ecosystem effects of ocean acidification. Nature, 454(7200): 96–99

Hawks J, Wang E T, Cochran G M, Harpending H C, Moyzis R K (2007). Recent acceleration of human adaptive evolution. Proc Natl Acad Sci USA, 104(52): 20753–20758

He W H, Yin H F, Sheng G L, Zhou X G (2004). Comparison of Paleozoic-Mesozoic mass extinction with big erosion of current biodiversity. Earth Science—Journal of China Universlty of Geosciences, 29(3): 263–269

Heywood V H (1995). Global Biodiversity Assessment. Cambridge: Cambridge University Press, 258

Horita J, Zimmermann H, Holland H D (2002). Chemical evolution of seawater during the Phanerozoic: Implications from the record of marine evaporates. Geochim Cosmochim Acta, 66(21): 3733–3756

Hotinski R M, Bice K L, Kump L R, Najjar R G, Arthur M A (2001). Ocean stagnation and end-Permian anoxia. Geology, 29(1): 7–10

Huang X Y, Jiao D, Lu L Q, Xie S C, Huang J H, Wang Y B, Yin H F, Wang H M, Zhang K X, Lai X L (2007). The fluctuating environment associated with the episodic biotic crisis during the Permo-Triassic transition: Evidence from microbial biomarkers in Changxing, Zhejiang Province. Science in China (Series D), 50(7): 1052–1059

Intergovernmental Panel on Climate Change (IPCC) (2007). Climate change 2007: The physical science basis: Contribution of Working Group 1 to the Fourth Assessment Report of IPCC. Cambridge: Cambridge University Press

Jiang H S, Lai X L, Luo G M, Aldridge R, Zhang K, Wignall P (2007). Restudy of conodont zonation and evolution across the P/T Boundary at Meishan Section, Changxing, Zhejiang, China. Global Planet Change, 55(1–3): 39–55

Jin Y G, Wang Y, Wang W, Shang Q H, Cao C Q, Erwin D H (2000). Pattern of marine mass extinction near the Permian-Triassic boundary in South China. Science, 289(5478): 432–436

Key R M, Kozyr A, Sabine C L, Lee K, Wanninkhof R, Bullister J L, Freely R A, Millero F J, Mordy C, Peng T H (2004). A global ocean carbon climatology: Results from Global Data Analysis Project (GLODAP). Global Biogeochem Cycles, GB4031, 23

Knoll A H, Bambach R K, Payne J L, Pruss S, Fischer W (2007). Paleophysiology and end-Permian mass extinction. Earth Planet Sci Lett, 256(3–4): 295–313

Korte C, Kozur H W, Mohtat-Aghai P (2004). Dzhulfian to lowermost Triassic $\delta^{13}C$ record at the Permian/Triassic boundary section at Shahreza, Central Iran. Hallesches Jahrbuch der Geowissenschaften. B18: 73–78

Kozur H W (2007). Biostratigraphy and event stratigraphy in Iran around the Permian-Triassic Boundary (PTB): Implications for the causes of the PTB biotic crisis. Global Planet Change, 55(1–3): 155–176

Li R C, Gu Y S, Xie S C (2005). The impact on the ecology of lacustrine swamp from the isolated lake and river in the Middle part of Yangtse River. Journal of Central China Normal University(Natural Sciences), 12: 76–79

Liang H D (2002). End Permian catastrophic event of marine acidification by hydrated sulfuric acid: Mineralogical evidence from Meishan Section of South China. Science Bulletin, 47: 784–788 (in Chinese)

Luo G M, Huang J H, Xie S C, Wignall P B, Tang X Y, Huang X Y, Yin H F (2010). Relationships between carbon isotope evolution and variation of microbes during the Permian-Triassic transition at

Meishan Section, South China. International Journal of Earth Science, 99: 775–784

Melchin M J, Mitchell C E (1991). Late Ordovician extinction of the Graptoloidea. In: Barnes C R, Williams S H, eds. Advances in Ordovician geology. Geological Survey of Canada Paper 90–9: 143–156

Nielsen R (2006). The Little Green Handbook: Seven Trends Shaping the Future of Our Planet. New York: Picador, 354 ISBN 0-312-42581-3

Orr J C, Fabry V J, Aumont O, Bopp L, Doney S C, Feely R A, Gnanadesikan A, Gruber N, Ishida A, Joos F, Key R M, Lindsay K, Maier-Reimer E, Matear R, Monfray P, Mouchet A, Najjar R G, Plattner G K, Rodgers K B, Sabine C L, Sarmiento J L, Schlitzer R, Slater R D, Totterdell I J, Weirig M F, Yamanaka Y, Yool A (2005). Anthropogenic ocean acidification over the twenty-first century and its impact on calcifying organisms. Nature, 437(7059): 681–686

Parry M L, Canziani O F, Palutikof J P, van der Linden P J, Hanson C E (2007). Climate change 2007: Impacts, adaptation and vulnerability: contribution of Working Group II to the fourth assessment report of the Intergovernmental Panel on Climate Change (IPCC). Cambridge: Cambridge University Press, 7–22

Payne J L, Lehrmann D J, Wei J Y, Orchard M J, Schrag D P, Knoll A H (2004). Large perturbations of the carbon cycle during recovery from the end-permian extinction. Science, 305(5683): 506–509

Payne J L, Turchyn A V, Paytan A, Depaolo D J, Lehrmann D J, Yu M, Wei J (2010). Calcium isotope constraints on the end-Permian mass extinction. Proc Natl Acad Sci USA, 107(19): 8543–8548

Racki G (2003). End-Permian mass extinction: Oceanographic consequences of double catastrophic volcanism. Lethaia, 36(3): 171–173

Rampino M R, Prokoph A, Adler A (2000). Tempo of the end-Permian event: high-resolution cyclostratigraphy at the Permian–Triassic boundary. Geology, 28(7): 643–646

Retallack G J (2001). A 300-million-year record of atmospheric carbon dioxide from fossil plant cuticles. Nature, 411(6835): 287–290

Retallack G J (2002). Carbon dioxide and climate over the past 300Myr. Philosophical Transactoins, Royal Society of London, A, 360: 659–673

Sandberg P A (1983). An oscillating trend in Phanerozoic nonskeletal carbonate mineralogy. Nature, 305: 19–22

Sepkoski J J (1992). A compendium of fossil marine animal families, 2n ed. Milwaukee Public Museum Contributions in Biology and Geology, 83: 1–156

Sheldon N D (2006). Abrupt chemical weathering increase across the Permian-Triassic boundary. Palaeogeogr Palaeoclimatol Palaeoecol, 231(3–4): 315–321

Smith F D M, May R M, Pellew R, Johnson T H, Walter K R (1993). How much do we know about the current extinction rate? Trends Ecol Evol, 8(10): 375–378

Sonnerup R E, McNochol A P, Quay P D, Gammon R H, Bullister J L, Sabine C L, Slater R D (2007). Anthropogenic $\delta^{13}C$ changes in the North Pacific Ocean reconstructed using a multiparameter mixing approach (MIX). Tellus B Chem Phys Meterol, 59(2): 303–317

Stanley G D (2001). The History and Sedimentology of Ancient Reef Systems. New York: Academic/Plenum Publishers

Steffen W, Sanderson A, Tyson P, Jager J, Matson P A, Moore III B, Oldfield F, Richardson K, Schellnhuber H J, Turner II B L, Wasson R J (2004). Global change and the Earth system: A planet under pressure: Executive summary of IGBP. Berlin: Springer-Verlag, 40

Tong J N, Zhang S X, Zuo J X, Xiong X Q (2007). Events during the Early Triassic recovery from the end-Permian extinction. Global Planet Change, 55(1): 66–80

Veizer J, Godderis Y, François L M (2000). Evidence for decoupling of atmospheric CO_2 and global climate during the Phanerozoic eon. Nature, 408(6813): 698–701

Visscher H, Brinkhuis H, Dilcher D L, Elsik W C, Eshet Y, Looy C V, Rampino M R, Traverse A (1996). The terminal Paleozoic fungal event: Evidence of terrestrial ecosystem destabilization and collapse. Proc Natl Acad Sci USA, 93(5): 2155–2158

Visscher H, Looy C V, Collinson M E, Brinkhuis H, van Konijnenburg-van Cittert J H, Kürschner W M, Sephton M A (2004). Environmental mutagenesis during the end-Permian ecological crisis. Proc Natl Acad Sci USA, 101(35): 12952–12956

Wang C J (2007). Anomalous hopane distributions at the Permian–Triassic boundary, Meishan, China: Evidence for the end-Permian marine ecosystem collapse. Org Geochem, 38(1): 52–66

Wang Y B, Tong J N, Wang J S, Zhou X G (2005). Calcimicrobialite after end-Permian mass extinction in South China and its palaeoenvironmental significance. Chin Sci Bull, 50(7): 665–671 (in Chinese)

Ward P D, Montgomery D R, Smith R (2000). Altered river morphology in south africa related to the permian-triassic extinction. Science, 289 (5485): 1740–1743

Wilson E O (1992). The Diversity of Life. Cambridge: Mass, Belknap Press of Harvard University Press, 468

Wilson E O (2002). The Future of Life. Vintage: Random House, 229

Wootton J T, Pfister C A, Forester J D (2008). Dynamical patterns and ecological impacts of changing ocean pH in a high-resolution multi-year dataset. Proc Natl Acad Sci USA, 105(48): 18848–18853

Xie S C, Guo J Q, Huang J H, Chen F, Wang H, Farrimond P (2004a). Restricted utility of ^{13}C of bulk organic matter as a record of paleovegetation in some loess-paleosol sequences in the Chinese Loess Plateau. Quat Res, 62(1): 86–93

Xie S C, Nott C J, Avsejs L A, Maddy D, Chambers F, Evershed R (2004b). Molecular and isotopic stratigraphy in an ombrotrophic mire for paleoclimate reconstruction. Geochim Cosmochim Acta, 68(13): 2849–2862

Xie S C, Pancost R D, Huang X Y, Jiao D, Lu L, Huang J, Yang F, Evershed R (2007). Molecular and isotopic evidence for episodic environmental change across the Permo/Triassic boundary at Meishan in South China. Global Planet Change, 55(1–3): 56–65

Xie S C, Pancost R D, Yin H F, Wang H, Evershed R P (2005). Two episodes of microbial change coupled with Permo/Triassic faunal mass extinction. Nature, 434(7032): 494–497

Yan J X, Wu M (2006). Synchronized osciliations in Phanerozoic chemical composition of seawater, carbonate sedimentation and biotic evolution: progresses and prospects. Geological Science and Technology Information, 25(3): 1–7 (in Chinese with English abstract)

Yang Z Y, Wu S B, Yin H F, Xu G R, Zhang K X, Bi X M (1993). Permo-Triassic Events of South China. Beijing: Geological Publishing House, 153

Yin H F, Feng Q L, Lai X L, Baud A, Tong J N (2007). The protracted Permo-Triassic crisis and the multi-episode extinction around the Permian-Triassic boundary. Global Planet Change, 55(1–3): 1–20

Yin H F, Huang S J, Zhang K X, Hansen H J, Yang F Q, Ding M H, Bi X M (1992). The effects of volcanism on the Permo-Triassic mass extinction in South China. In: Sweet W C, Yang Z Y, Dickins J M, Yin H F, eds. Permo-Triassic Events in the Eastern Tethys. Cambridge: Cambridge University Press, 169–174

Yu J X, Peng Y Q, Zhang S X, Yang F Q, Zhao Q M, Huang Q S (2007). Terrestrial events across the Permian-Triassic boundary along the Yunnan-Guizhou border, SW China. Global Planet Change, 55(1–3): 193–208

Hongfu YIN, professor of China University of Geosciences (CUG), Member of the Academy of China, Deputy Director of the National Committee of Stratigraphy; Vice-chairman of the Subcommittee of Triassic Stratigraphy, International Committee of Stratigraphy (2000–2008). Awards: Three 2nd class National Natural Science Awards (1999, 2002, 2008) and othes. His main works concentrated in paleontology and geobiology. He was the editor of “The Palaeobiogeography of China”, the English edition of which was published in Oxford Biogeography Series. He led the international investigation of the Permian-Triassic Boundary research and finally succeeded in establishment of the Global PTB Stratotype in Changxing, Zhejiang Province. His group leads the geobiological research in China. Publications: 240 academic papers and 24 books.

Dr. Weihong HE, Professor of China University of Geosciences, was born in 1971, graduated from China University of Geosciences in 1996 and received her doctoral degree at China Institute of Geosciences, Beijing, China in 2002. Her research interests involve brachiopods, radiolarians, Claraia (Bivalva), ammonites as well as palaeoecology.
Email: whzhang@cug.edu.cn

Shucheng XIE has a BA degree in geology and a PhD in paleontology and stratigraphy from China University of Geosciences (Wuhan) in 1989 and 1997, respectively. With a special interest in geolipids, in particular the biomarkers, he has launched a survey covering a broad range of sediments in the Earth history including ice-cores and snow, loess-paleosol sequences, peat deposits, speleothems and lacustrine sediments, and marine sedimentary rocks. By exploring these biomarker fingerprints, in particular those from microbes, he is able to trace the paleo-environmental change and the biotic crisis. His current work focuses on the three critical periods, i.e., Quaternary, Permian-Triassic transition and Mesoproterozoic. Now, he has the research orientation of geobiology, organizing the international conference of geobiology and co-chairing with professor Roger Summons from MIT the geomicrobiology session in the third international paleontology congress in 2010. He set up the biomarker laboratory in the university equipped with the facilities of GC, GC/MS, LC/MS, GC-C-IRMS and GC-TC-IRMS. Due to his achievements in geolipids, he got the outstanding postdoctorate award in 2005 and the second prize of the national award for natural science in 2008.